



HAL
open science

Interpenetrated Constitutional Networks of Aromatic Metallosupramolecular Duplexes

Yves-Marie Paul Legrand, Florina Dumitru, Arie van Der Lee, Mihail Barboiu

► **To cite this version:**

Yves-Marie Paul Legrand, Florina Dumitru, Arie van Der Lee, Mihail Barboiu. Interpenetrated Constitutional Networks of Aromatic Metallosupramolecular Duplexes. *Supramolecular Chemistry*, 2009, 21 (03-04), pp.230-237. 10.1080/10610270802478271 . hal-00513542

HAL Id: hal-00513542

<https://hal.science/hal-00513542v1>

Submitted on 1 Sep 2010

HAL is a multi-disciplinary open access archive for the deposit and dissemination of scientific research documents, whether they are published or not. The documents may come from teaching and research institutions in France or abroad, or from public or private research centers.

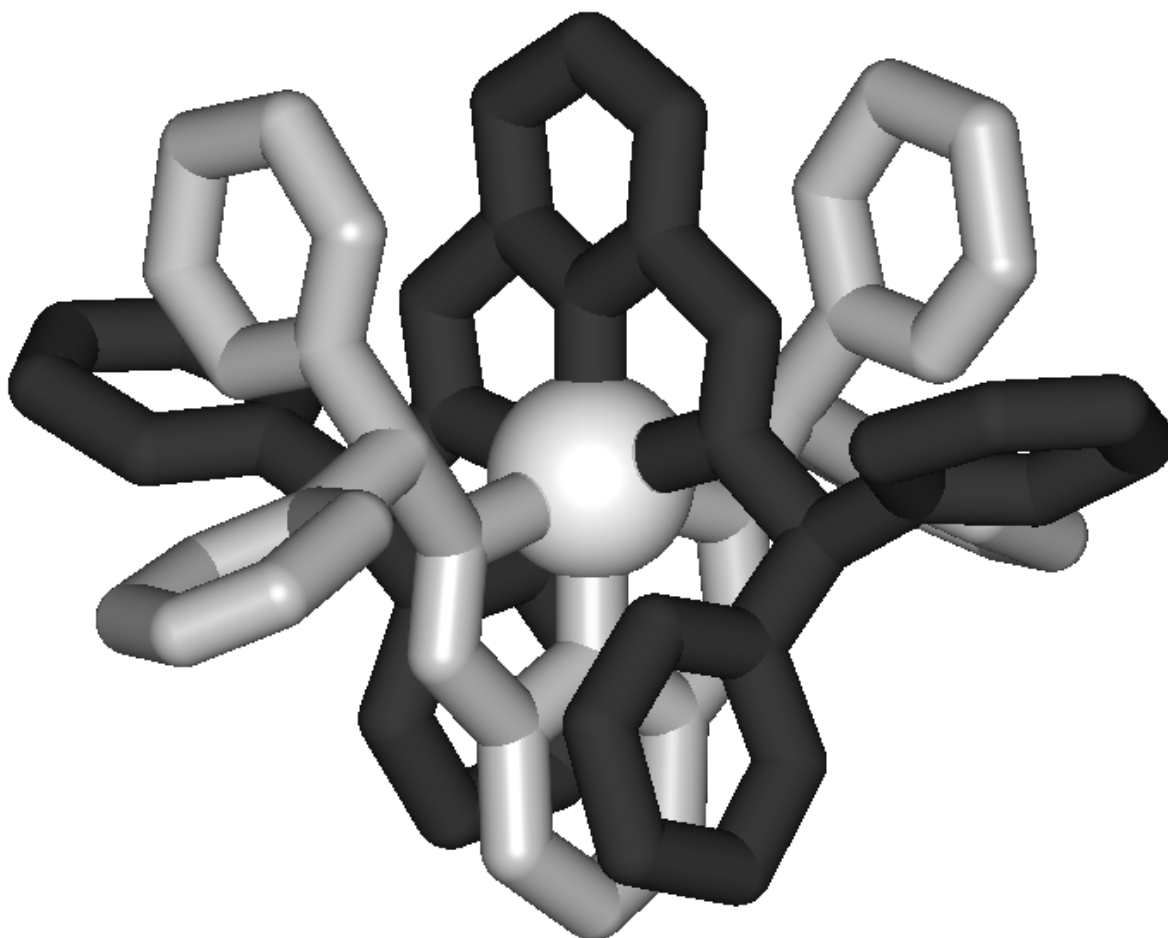
L'archive ouverte pluridisciplinaire **HAL**, est destinée au dépôt et à la diffusion de documents scientifiques de niveau recherche, publiés ou non, émanant des établissements d'enseignement et de recherche français ou étrangers, des laboratoires publics ou privés.



Interpenetrated Constitutional Networks of Aromatic Metallosupramolecular Duplexes

Journal:	<i>Supramolecular Chemistry</i>
Manuscript ID:	GSCH-2008-0078.R1
Manuscript Type:	Full Paper
Date Submitted by the Author:	26-Aug-2008
Complete List of Authors:	Legrand, Yves-Marie; Institut Europeen des Membranes Dumitru, Florina; Institut Europeen des Membranes van der Lee, Arie; Institut Europeen des Membranes Barboiu, Mihail; Institut Européen des Membranes
Keywords:	metallosupramolecular complexes, imine, self-assembly, aromatic interactions
<p>Note: The following files were submitted by the author for peer review, but cannot be converted to PDF. You must view these files (e.g. movies) online.</p> <p>2Zn2.cif 3Zn2.cif 4Zn2.cif Scheme1a.cdx Scheme1b.cdx Scheme1c.cdx</p>	





view Only

1
2
3
4
5
6
7
8
9
10
11
12
13
14
15
16
17
18
19
20
21
22
23
24
25
26
27
28
29
30
31
32
33
34
35
36
37
38
39
40
41
42
43
44
45
46
47
48
49
50
51
52
53
54
55
56
57
58
59
60

Interpenetrated Constitutional Networks of Aromatic Metallosupramolecular Duplexes

Y.-M. LEGRAND^a, F. DUMITRU^{a, b}, A. V. D. LEE^a & M. BARBOIU^{a,*}

^a*Institut Européen des Membranes, Adaptive Supramolecular Nanosystems Group - ENSCM-UMII-CNRS UMR- 5635, Place Eugène Bataillon, CC 047, F-34095 Montpellier, Cedex 5, France,* ^b*University “Politehnica” of Bucharest, Department of Inorganic Chemistry, 1, Polizu st., RO-011061 Bucharest, Romania¹*

We report hierarchical supramolecular organization promoted by the formation of metallosupramolecular duplex architectures. 3D supramolecular structure propagation is favoured by long-range aromatic-aromatic interactions toward robust double-helical configuration in 1_2Zn^{2+} , tubular squared architecture in 2_2Zn^{2+} and self-organized triangles in 4_2Zn^{2+} . The advantageous structural features of such external aromatic interactions are not preserved while introducing new variables such as methylene spacer between imine moiety and the aromatic rings, inducing a orthogonal spatial orientation of the peripheral aromatic arms in 3_2Zn^{2+} . Indeed, the introduction of supplementary aromatic functionality in 4_2Zn^{2+} , results in the combination of both internal and external forces and has led to metallosupramolecular triangle architectures that are stabilized by 3D “diphenylmethane embrace motifs”. The homochiral triangles connected via tetrahedral nodes and face-to-face triangle interactions are organized in the crystal that each duplex constituent has an alternate opposite chirality

Keywords: metallosupramolecular complexes, imine, self-assembly, aromatic interactions

Corresponding author. E-mail: mihai.barboiu@iemm.univ-montp2.fr

INTRODUCTION

Molecular self-organisation is the basis for the construction of new useful synthetic materials in a bottom-up strategy. The way from molecular to nano(micro)-scale systems depend both on the nature of its constituents and on the interactions between them.[1-4]. The self-organization exploits non-covalent interactions in a multitude of ways and implements sets of molecules containing specific information stored in the arrangement of specific binding sites. The selection of one or more supramolecular architectures occurs as function of either internal (such as the nature and the geometry of the binding subunits, the composition, etc.) or external factors (such as the nature of the medium, the presence of specific molecules or anions, etc). Metal-directed self-assembly [3-5] or combined hydrogen-bonding-metal coordination [6] and π - π stacking-metal coordination [7] supramolecular interactions has been extensively used as a powerful tool for the spontaneous generation of such nanostructures.

We have recently reported the double helical complex 1_2Zn^{2+} (Fig.1a) which after being left to stand for some hours produced homochiral crystals containing only one of Δ and Λ mirror enantiomers. [8] In the crystal of 1_2Zn^{2+} each duplex of one helical sense is π - π stacked with two duplexes of the same helical sense (Fig.1b). This pattern generates double helix stacks of 1_2Zn^{2+} units. In the crystal the adjacent columns of one helical sense run in parallel directions and interweave the peripheral phenyl and pyridine rings which are in van der Waals contact in a one-over/one-under fashion (Fig.1c). This generates a gearwheels-type mechanism with a very uncommon topology such that each double helix is in van der Waals contact with four neighbouring ones of the same helical sense.

A set of interconverting Δ and Λ mirror enantiomers of 1_2Zn^{2+} units represents a constitutional dynamic library [8c, d] in solution. After some hours, single-crystals started to form in the acetonitrile/*i*-propylether system and resolved homochiral metallosupramolecular domains of unique helicity had been amplified through a phase-change driven selection

1
2
3 process. [8d] Constitutional affinity drives the selection of interdigitated homochiral double-
4
5 helical architectures under internal pressure of the 3D long range multiscrew-type interactions
6
7 (Fig.1d). Weak aromatic interactions, stabilize such supramolecular assemblies by π -stacking
8
9 and van der Waals aromatic interactions and constitute the driving force of the homochiral
10
11 crystal phase cohesion.
12
13

14
15 Figure 1 here

16
17
18 Scheme 1 here

19
20 To obtain systematic insights into the creation of these architectures interacting via
21
22 peripheral aromatic groups which are responsible for the constitutional communication
23
24 between homochiral double-helical columns within the 3D crystalline space, we investigated
25
26 new similar systems by combining metal-ion coordination with weak aromatic-aromatic
27
28 interactions. As a step towards this goal, it is of interest to investigate whether changes in
29
30 expression of the crystal packing can be modulated by considering *outer structural factors*, by
31
32 introducing different aromatic substituents on the peripheral surface. One possible
33
34 presumption is to consider that the additional supramolecular aromatic interactions like in
35
36 biphenyl-type compound **2** or different spatial orientation of phenyl moiety like in the benzyl-
37
38 type compound **3** or supplementary hydrophobic interactions in the bisphenylmethane-type
39
40 compound **4** might direct the constitutional organisation of the crystalline frameworks by
41
42 controlling the supramolecular connectivity between the ligands of the metallosupramolecular
43
44 duplexes 2_2Zn^{2+} , 3_2Zn^{2+} and 4_2Zn^{2+} (Scheme 1).
45
46
47
48
49
50
51
52

53 EXPERIMENTAL SECTION

54
55 **Materials and Methods:** 2,6-pyridinedicarboxaldehyde was prepared by oxidation of
56
57 2,6-pyridinemethanol with activated MnO_2 according to the procedure described in the
58
59 literature [11a]. 4-aminobiphenyl, benzylamine, benzhydramine were purchased from
60

1
2
3 Aldrich and used as received. All other reagents were obtained from commercial suppliers
4
5 and used without further purification. All organic solutions were routinely dried by using
6
7 sodium sulfate (Na_2SO_4). ^1H and ^{13}C NMR spectra were recorded on an ARX 300 MHz
8
9 Bruker spectrometer in CDCl_3 with the use of the residual solvent peak as reference. The
10
11 assignments were made on the base of the COSY and NOESY spectra. Mass spectrometric
12
13 studies were performed in the positive ion mode using a quadrupole mass spectrometer
14
15 (Micromass, Platform II). Samples were continuously introduced into the mass spectrometer
16
17 through a Waters 616HPLC pump. The temperature (60°C) and the extraction cone voltage
18
19 ($V_c=5-10\text{V}$) were usually set to avoid fragmentations.
20
21
22
23
24
25
26

27 **Synthesis of ligands 1-4** : Ligand **1** [11] and **3** [12] were synthesised as previously described.

28
29 **Ligand 2** – has been synthesized in EtOH by condensation of 2,6-pyridinedicarboxaldehyde
30
31 (0.1g, 0.74 mmol) with 4-aminobiphenyl (0.25g, 1.48mmol), under reflux for 12 h with
32
33 constant stirring. After solvent evaporation, the resulting crude material was recrystallized
34
35 from acetonitrile to give **2** as a light-yellow solid, (0.275g, 85%). F.M. $\text{C}_{31}\text{H}_{23}\text{N}_3$,
36
37 MW=437.55 g/mol. ^1H -NMR (300Hz, CDCl_3 , ppm) : δ = 8.769 (s, 2H, CH=N), 8.347-8.321
38
39 (d, 2H, H^b , $J=7.8\text{Hz}$), 8.005-7.952 (t, 1H, H^a , $J=7.8\text{Hz}$), 7.696-7.632 (m, 8H, H^{c+d}), 7.488-
40
41 7.338 (m, 10H, H^{arom}). MS (ESI): m/z (100%): 438.25 (2-H^+).
42
43
44
45

46 **Ligand 4:** – has been synthesized in EtOH by condensation of 2,6-pyridinedicarboxaldehyde
47
48 (0.1g, 0.74 mmol) with benzhydramine (0.27g, 1.48mmol), under reflux for 12 h with
49
50 constant stirring. After solvent evaporation, the resulting crude material was recrystallized
51
52 from acetonitrile to give **4** as a white solid, (0.310 g, 90%). F.M. $\text{C}_{33}\text{H}_{27}\text{N}_3$, MW=465.59
53
54 g/mol. ^1H -NMR (300Hz, CDCl_3 , ppm) : δ = 8.530 (s, 2H, CH=N), 8.273-8.248 (d, 2H, H^b ,
55
56 $J=7.5\text{Hz}$), 7.848-7.796 (t, 1H, H^a , $J=7.8\text{Hz}$), 7.404-7.217 (m, 20H, H^{ar}), 5.700 (s, 2H, CH).
57
58 MS (ESI): m/z (100 %): 466.29 (4-H^+).
59
60

Synthesis and single crystal structures of 1_2Zn^{2+} - 4_2Zn^{2+} complexes. The reactions were performed typically on a 10 mg scale of ligand. The ligands **1-4** and $\text{Zn}(\text{CF}_3\text{SO}_3)_2$ were dissolved in CD_3CN (1 mL), and stirred overnight at 60 °C. Layering such solutions duplex complexes 1_2Zn^{2+} - 4_2Zn^{2+} in acetonitrile with the *i*-propylether at room temperature, resulted in a unique set of single-crystals suitable for X-ray single-crystal experiments.

Compound 1_2Zn^{2+} : $^1\text{H-NMR}$ (CD_3CN , ppm) : δ = 8.82 (s, 4H, CH=N), 8.60-8.55 (t, 2H, H^a , $J=7.8$ Hz), 8.27-8.24 (d, 4H, H^b , $J=7.8$ Hz), 7.38-7.25 (m, 12H, H^{ar} , $J=8.7$ Hz), 6.91-6.88 (d, 8H, H^{ar} , $J=3.35$ Hz). ES-MS: m/z (%): 317.7 (100)

Compound 2_2Zn^{2+} : $^1\text{H-NMR}$ (CD_3CN , ppm) : δ = 8.901 (s, 4H, CH=N), 8.626-8.574 (t, 2H, H^a , $J=7.8$ Hz), 8.297-8.271 (d, 4H, H^b , $J=7.8$ Hz), 7.631-7.414 (m, 32H, $\text{H}^d+\text{H}^{\text{ar}}$, $J^{d-c}=8.4$ Hz), 6.923-6.895 (d, 8H, H^c , $J^{c-d}=8.4$ Hz). ES-MS: m/z (%): 469.46 (100)

Compound 3_2Zn^{2+} : $^1\text{H-NMR}$ (CDCl_3 , ppm) : δ = 8.62-8.58 (t, 2H, H^a , $J=7.8$ Hz), 8.05 (s, 2H, CH=N), 7.85-7.80 (d, 2H, H^b), 7.20-7.10 (t, 2H, H^{ar}), 7.05-6.95 (t, 4H, H^{ar}), 6.65-6.55 (d, 4H, H^{arom}), 4.60 (s, 8H, CH_2). ES-MS: m/z (%): 373.7 (100)

Compound 4_2Zn^{2+} : $^1\text{H-NMR}$ (CD_3CN , ppm) : δ = 8.244-8.192 (t, 2H, $J=7.8$ Hz), 7.935/7.927* (s, 4H, CH=N), 7.692-7.666 (d, 4H, $J=7.8$ Hz), 7.210-7.112 (m, 40H, H^{ar}), 5.548/5.540* (s, 4H, CH). ES-MS: m/z (%):497.54 (100).* *atropisomerism at room temperature see text.*

X-ray Single Crystal Diffraction Data for 1_2Zn^{2+} - 5_2Zn^{2+} , 1_2Fe^{2+} and 1_2Co^{2+} complexes:

The diffraction intensities were collected at the joint X-ray Scattering Service of the Institut Charles Gerhardt and the Institut Européen des Membranes of the University of Montpellier II, France, at 175 K using an Oxford Diffraction Xcalibur-I and a Gemini-S diffractometer. The crystal-to-detector distance was 50 mm for all five measurements. The structures were solved by direct methods using SIR2002 [13a] or by ab-initio (charge-flipping) methods using SUPERFLIP [13b] and refined by least-squares methods on F using CRYSTALS [13C],

1
2
3 against $|F|$ on data having $I > 2\sigma(I)$; R -factors are based on these data. Hydrogen atoms were
4
5 partly located from difference Fourier synthesis, partly placed based on geometrical
6
7 arguments, and in general not refined. Non-hydrogen atoms were in general refined
8
9 anisotropically, except where the data to parameter ratio did not allow doing this. Full details
10
11 can be found in the cif-files and in Supplementary material.
12
13
14

15
16 Crystallographic data (excluding structure factors) for the structures reported in this paper
17
18 have been deposited with the Cambridge Crystallographic Data Centre as supplementary
19
20 publication no. CCDC-695886-695888. Copies of the data can be obtained free of charge on
21
22 application to CCDC, 12 Union Road, Cambridge CB2 1EZ, UK (fax: (+44) 1223 336-033; e-
23
24 mail: deposit@ccdc.cam.ac.uk).
25
26
27
28

29 30 RESULTS AND DISCUSSION

31
32 The crystal structures of the complexes 2_2Zn^{2+} , 3_2Zn^{2+} and 4_2Zn^{2+} were determined from
33
34 crystals obtained from the acetonitrile/*i*-propylether solutions at room temperature. The
35
36 molecular and the crystal packing structures are presented in Figures 2 and 3. In all duplex
37
38 structures 2_2Zn^{2+} , 3_2Zn^{2+} and 4_2Zn^{2+} the Zn^{2+} ions are fully coordinated by two ligands
39
40 arranged into two orthogonal planes and present an octahedral coordination geometry (Fig. 2).
41
42 The average $\text{Zn}^{2+}\text{-N}_{\text{Pyridine}}$, $\text{Zn}^{2+}\text{-N}_{\text{imine}}$ and $\text{Zn}^{2+}\text{-N}_{\text{imine}}$, distances are 2.05 or 2.24 Å,
43
44 respectively.
45
46
47
48

49
50 Figure 2 here

51
52 The unit cell of 2_2Zn^{2+} was found to contain six homoduplex complexes together with
53
54 twelve triflate counterions. Overall the crystal structure is racemic and the duplexes are
55
56 organized in parallel layers of Δ and Λ mirror enantiomers which are alternatively stratified.
57
58 Within a layer they are associated by two different sets of π - π stacking interactions (Fig.3a).
59
60

Figure 3 here

1
2
3 These aromatic stacking interactions are constitutionally different and allow in one
4 direction the internal overlaps between the biphenyl-pyridine triads with the average centroid-
5 centroid distances of 3.71 and 3.98 Å corresponding to van der Waals contact. The terminal
6
7
8 centroid distances of 3.71 and 3.98 Å corresponding to van der Waals contact. The terminal
9
10 phenyl moiety of the biphenyl triad in further π - π stacked with a similar one of the adjacent
11
12 layer (the average centroid-centroid distance of 3.94 Å). In the other direction, each layer is
13
14 alternatively stratified above each other by stacking only the terminal biphenyl moieties, such
15
16 that each layer is in van der Waals contact (the average centroid-centroid distance of 4.10 Å).
17
18 The square packing arrangement of duplex subunits results in the formation of a tubular
19
20 structure with a hydrophobic hole of approximately 3 Å. The triflate anions are arranged into
21
22 approximately linear array tightly fitting into the central cavity of the resulted tubular
23
24 channels (Fig.3b).
25
26
27
28

29 Figure 4 here
30

31
32 As expected, the solution studies revealed that the introduction of the methylene
33
34 spacer between the imine moiety and the terminal phenyl moieties dramatically change the
35
36 spatial orientation of the phenyl moieties. The signals of the phenyl moieties of the complex
37
38 3_2Zn^{2+} were overall strongly shielded ($\Delta\delta = 1.0$) with respect to the ligand **3**, suggesting
39
40 strong intramolecular attractive π - π stacking interactions between the phenyl and central
41
42 pyridine moiety.
43
44
45

46 The unit cell of the complex 3_2Zn^{2+} was found to contain four duplex complexes
47
48 together with eight triflate counterions. In the crystal the two ligands are strongly intertwined
49
50 stabilizing the duplex superstructure by internal π - π stacking interactions (Fig. 2c). The
51
52 relative position of the duplex ligands allows an internal overlap between the phenyl moieties
53
54 and the central pyridine moiety with an average centroid-centroid distance of 3.9 Å
55
56 corresponding to a van der Waals contact. In the crystal the communication between duplexes
57
58 3_2Zn^{2+} is disrupted, each duplex being closely packed with the two neighbouring ones by
59
60

1
2
3 weak van der Waals contacts (Fig. 4). It is useful to briefly emphasize the influence of the
4
5 introduction of the methylene spacer which is clearly important for internal holding and
6
7 stabilizing the duplex formation by the π - π stacking. However the external π - π stacking
8
9 communication is completely removed and non-communicating duplex structures are present
10
11 in the crystal structure. Overall the crystal structure is racemic and Δ and Λ mirror
12
13 enantiomers duplexes are closely packed via van der Waals contacts.
14
15

16
17
18 Compared with 1_2Zn^{2+} duplex with an intermediate orientation of the terminal phenyl
19
20 rings allowing internal and external π - π stacking interactions, the external aromatic
21
22 interactions are completely suppressed in the 3_2Zn^{2+} framework and further substitution of the
23
24 methylene moiety in **3** with a second phenyl moiety in ligand **4** would result in external
25
26 structural communication between the multiaromatic duplexes 4_2Zn^{2+} .
27
28

29
30 The free rotation of the diphenylmethane groups around CH-N bond is possible in
31
32 *cisoid-cisoid* [5f] conformation of the ligand **4** and one singlet was identified in ^1H -NMR
33
34 spectrum. Two sets of singlet signals were identified in the regions of 7.9 and 5.5 ppm of ^1H -
35
36 NMR spectrum of 4_2Zn^{2+} for imine and CH protons, indicating a hindered rotation of the four
37
38 diphenylmethane groups sterically very close to the neighbouring ones (see Fig. 2d) when
39
40 4_2Zn^{2+} duplexes form in the presence of the Zn^{2+} metal ions. On account of the hindered
41
42 rotation of diphenylmethane groups around CH-N bond in the 4_2Zn^{2+} duplex, the two sets of
43
44 signals in the ^1H -NMR spectrum can be assigned to the Δ and Λ mirror atropenantiomers.
45
46
47 (Supporting informations)
48
49

50
51 Figure 5 here
52

53
54 The unit cell of 4_2Zn^{2+} complex was found to contain sixteen duplex complexes
55
56 together with thirty-two very disordered triflate counterions and filling the interstices between
57
58 the duplexes so that all available space is filled. Symmetry expansion of the crystal cell of
59
60 4_2Zn^{2+} shows that the self-assembly of the duplex units form triangle-like trimers. Three

1
2
3 duplexes of the same chirality are self-assembled into a metallosupramolecular triangle that is
4
5 stabilized by a new three-dimensional “diphenylmethane embrace trimer” in which three V-
6
7 shaped bisaromatic units fill their interstices so that their internal available space is filled (Fig.
8
9 5a). Aromatic embrace motifs are well documented for a series of aromatic clusters [10] and
10
11 their significance in terms of interactions (for example stabilization energy of the benzene
12
13 trimer is estimated to be -20 KJ/mol) is widely recognized [14]. Diphenylbenzene trimers
14
15 formation in the solid state has been previously reported. [15] The diphenylmethane embrace
16
17 trimerization in 4_2Zn^{2+} may contribute to the stabilization of such hierarchically self-
18
19 assembled duplexes. The crystal structure is racemic. The homochiral triangles connected via
20
21 tetrahedral nodes and face-to-face triangle interactions are organized in the crystal that each
22
23 duplex constituent has an alternate opposite chirality (Fig 5b).
24
25
26
27

28 29 CONCLUSION

30
31 In conclusion we have demonstrated in this paper the synthesis of large solid state
32
33 supramolecular crystalline superstructures stitched together from a combination of metal-
34
35 coordination and weak π - π stacking and van der Waals aromatic interactions. Hierarchical
36
37 supramolecular organization is promoted by the formation of metallosupramolecular duplex
38
39 architectures stabilized by internal π - π stacking interactions and by long-range
40
41 supramolecular spatial interactions between duplex systems via specific aromatic interactions.
42
43 Long-range 3D supramolecular structure propagation is favoured via weak internal stacking
44
45 interactions toward robust double-helical configurations in 1_2Zn^{2+} , tubular squared packed
46
47 architecture in 2_2Zn^{2+} and homochiral triangles in 4_2Zn^{2+} . The advantageous structural
48
49 features of such external interactions are not preserved while introducing new variables such
50
51 as methylene spacer between imine moiety and phenyl groups, inducing a very different
52
53 spatial orientation of the lateral aromatic arms in 3_2Zn^{2+} . This configuration is clearly
54
55 important for internal holding and stabilize the duplex formation by the π - π stacking.
56
57
58
59
60

1
2
3 However the external π - π stacking interactions are completely removed and non-
4 communicating duplex structures are present in the crystal structure of 3_2Zn^{2+} . Indeed, the
5 introduction of supplementary aromatic functionality results in the combination of both
6 internal and external forces and has led to metallosupramolecular triangle architectures that
7 are stabilized by is stabilized by a new three-dimensional “diphenylmethane embrace motif”.

8
9
10 The use of such multiple hierarchical aromatic interactions provide a very powerful
11 tool and a target supramolecular platform for the stabilization of constitutional tertiary
12 superstructures but also for a kind of modulable structure in the presence of external stimuli.
13 Functional supramolecular devices for gas storage or catalysts are envisaged for the systems
14 reported here and such studies are underway.

15 16 17 18 19 20 21 22 23 24 25 26 27 28 *Acknowledgements*

29
30
31 This work, conducted as part of the award “Dynamic adaptive materials for separation and
32 sensing Microsystems” (M.B.) made under the European Heads of Research Councils and
33 European Science Foundation EURYI (European Young Investigator) Awards scheme in
34 2004, was supported by funds from the Participating Organizations of EURYI and the EC
35 Sixth Framework Program. See www.esf.org/euryi. This research was also supported in part
36 by the ANR-06-Blan-0117 POLYFUNMAG Program and CNRS.

37 38 39 40 41 42 43 44 *References*

- 45 1. a) Lehn, J.-M. *Supramolecular Chemistry-Concepts and Perspectives*, VCH, Weinheim,
46 **1995**, pp124-138; (b) Lehn, J.-M. *Proc. Natl. Acad. Sci.* **2002**, *99*, 4763-4768.
47
- 48 2. *J. Chem. Soc., Dalton Trans.* **2000**, *21*, Special Issue on Crystal Engineering.
49
- 50 3. For recent reviews on metal ion metal self-assembly, see for exemple: (a) Leininger, S.,
51 Olenyuk; B., Stang, P.J. *Chem. Rev.* **2000**, *100*, 853-908; (b) Swiegers, G.F.; Malfetese, T.F.
52
53 *Chem. Rev.* **2000**, *100*, 3483-3538; (c) Holliday, B.J.; Mirkin, C.A. *Angew. Chem.* **2001**, *113*,
54
55 2076-2097, *Angew. Chem. Int. Ed.*, **2001**, *40*, 2022-2043.
56
57
58
59
60

- 1
2
3
4
5
6
7
8
9
10
11
12
13
14
15
16
17
18
19
20
21
22
23
24
25
26
27
28
29
30
31
32
33
34
35
36
37
38
39
40
41
42
43
44
45
46
47
48
49
50
51
52
53
54
55
56
57
58
59
60
4. For recent reviews on metal hydrogen-bonding self-assembly, see for exemple: (a) Desiraju, G.R. *Acc. Chem. Res.*, **2002**, *35*, 565-573 b) Lehn, J.-M. in *Supramolecular Polymers*, ed. Ciferri, A. Dekker, New York, NY, **2000**, 615-641; (c) Archer, E.A.; Gong, H.; Krische, M. J. *Tetrahedron* **2001**, *57*, 1139-1159.
5. a) Schmuck, C. *Angew. Chem.* **2003**, *115*, 2552-2556, *Angew. Chem. Int. Ed.* **2003**, *42*, 2448-2451; b) OH, K.; Jeong, K.-S.; Moore, J. S. *Nature* **2001**, *414*, 889-893; c)
6. a) Braga, D.; *J. Chem. Soc., Dalton Trans.* **2000**, *21*, 3705-3713; b) Noveron, J.C.; Lah, M.S.; del Sesto, R.E.; Arif, A.M.; Miller, J.S.; Stang, P.S. *J. Am. Chem. Soc.* **2002**, *124*, 6613-6625; c) Uemura, K. S.; Kitagawa, M.; Kondo, K.; Fukui, R.; Kitaura, H. C.; Chang, T.; Mizutani, T. *Chem. Eur. J.* **2002**, *8*, 3587-3600; d) Tadokoro, M.; Kanno, H.; Kitajima, T.; Shimada, H.; Nakanishi, N.; Isodobe, K.; Nakasuji, K. *Proc. Natl. Acad. Sci.* **2002**, *99*, 4950-4995; e) Muthu, S.; Yip, J.H.K.; Vittal, J.J.; *J. Chem. Soc., Dalton Trans.* **2002**, *23*, 4561-4568 f) Barboiu, M.; Lehn, J.-M. *Proc. Natl. Acad. Sci. USA* **2002**, *99*, 5201-5206; g) Barboiu M.; Cerneaux, S.; van der Lee, A.; Vaughan, G. *J. Am. Chem. Soc.* **2004**, *126*, 3545-3550; h) Cazacu, A.; Tong, C.; van der Lee, A.; Fyles, T. M.; Barboiu, M. *J. Am. Chem. Soc.* **2006**, *128*, 9541-9548; i) Arnal-Herault, C.; Michau, M.; Pasc-Banu, A.; Barboiu, M. *Angew. Chem. Int. Ed.*, **2007**, *46*, 4268-4272; (k) Arnal-Herault, C.; Pasc-Banu, A.; Michau, M.; Cot, D.; Petit, E.; Barboiu, M. *Angew. Chem. Int. Ed.* **2007**, *46*, 8409-8413; (l) Michau, M.; Barboiu, M.; Caraballo, R. Arnal-Hérault, C.; Periat P.; van der Lee, A.; Pasc, A. *Chem. Eur.J.*, **2008**, *14*, 1776-1783 m) Barboiu, M.; Supuran, C.T.; Menabuoni, L. ; Scozzafava, A.; , Mincione, F.; Briganti, F.; Mincione, G. *J. Enzymol. Inhib.*, **1999**, *15*, 23-46; n) Barboiu, M.; Guizard, C.; Hovnanian, N.; Palmeri, J.; Reibel, C.; Luca, C.; Cot, L. *J. Membrane Sci.*, **2000**, *172*, 91-103; o) Barboiu, M.; Guizard, C.; Luca, C.; Hovnanian, N.; Palmeri, J.; Cot, L. *J. Membrane Sci.*, **2000**, *174*, 277-286; p) Villamo, O.; Barboiu, C.; Barboiu, M.; Yau-Chun-Wan, W.; Hovnanian, N. *J. Memb. Sci.*, **2002**, *204*, 97-110.

- 1
2
3 7. a) Barboiu, M.; Lehn, J.-M. *Revista de Chimie*. **2006**, *9*, 909-914; b) Barboiu, M.; Vaughan,
4 G.; Kyritsakas, N.; Lehn, J.-M. *Chem. Eur J.* **2003**, *9*, 763-769; c) Barboiu, M.; Petit, E.;
5 Vaughan, G. *Chem. Eur. J.* **2004**, *10*, 2263-2270; d) Blondeau, P.; van der Lee, A.; Barboiu,
6 M. *Inorg. Chem.* **2005**, *44*, 5649-5653 e) Barboiu, M.; Lehn, J.M. *Revista de Chimie*, **2008**
7 *i59(3)*, 255-259.
8
9
10
11
12
13
14
15 8. a) Dumitru, F.; Petit, E.; van der Lee, A.; Barboiu, M. *Eur. J. Inorg. Chem.* **2005**, *21*, 4255-
16 4262; b) Legrand, Y.M.; van der Lee, A.; Barboiu, M. *Inorg. Chem.* **2007**, *46*, 9540-9547; c)
17 Lehn, J. M. *Chem. Soc. Rev.* **2007**, *36*, 151-160; d) Angelin, M.; Fischer, A. & Ramstrom, O.
18 *J. Org. Chem.* **2008**, *73*, 3593-3595.
19
20
21
22
23
24
25 9. Scudder, M.L.; Goodwin, H.A.; Dance, I.G. *New J. Chem.* **1999**, *23*, 695-705.
26
27
28
29 10. Lions F.; Martin, K. V. *J. Am. Chem. Soc.*, **1957**, *79(11)*, 2733-2738.
30
31
32 11. a) Vance, A.L.; Alcock, N.A.; Heppert, J.A.; Busch, D. H. *Inorg. Chem.* **1998**, *37*, 6912-
33 6920; b) de Bruin, B.; Bill, E.; Bothe, E.; Weyhermüller, T.; Wieghardt, K. *Inorg. Chem.*
34 **2000**, *39*, 2936-2947.
35
36
37 12. Creber, M.L.; Orrell, K.G.; Osborne, A.G.; Sik, V.; Bingham, A. L.; Hursthouse, M.B. *J.*
38 *Organomet. Chem.* **2001**, *631*, 125-134.
39
40
41 13. a) Burla, M. C.; Camalli, M. B.; Carrozzini, G. L.; Cascarano, R.; Giacovazzo, C.;
42 Polidori, G.; Spagna, R. *J. Appl. Crystallogr.*, **2003**, *36*, 1103; (b) Betteridge, P. W.;
43 Carruthers, J. R.; Cooper, R. I.; Prout, K.; Watkin, D. J. *J. Appl. Crystallogr.*, **2003**, *36*, 1487.
44
45 (c) Palatinus, L.; Chapuis, G. *J. Appl. Cryst.* **2007**, *40*, 786-790
46
47
48
49
50 14. Morimoto, T.; Uno, H.; Furuta, H. *Angew. Chem. Int. Ed.*, **2007**, *46*, 3672-3675.
51
52
53 15. a) Kusukawa, T.; Fujita, M. *J. Am. Chem. Soc.* **2006**, *124*, 13576. b) Mislow, K. *J. Org.*
54 *Chem.* **1981**, *46*, 4975; b) Precigoux, G.; Barrans, Y.; Busetta, B.; Marsau, P. *Acta*
55 *Crystallogr., Sect. B: Struct. Crystallogr. Cryst. Chem.* **1975**, *31*, 1497.
56
57
58
59
60

Figure caption

FIGURE 1. From achiral ligands to metallosupramolecular homochiral double helical strands.

a) Synthesis of 1_2Zn^{2+} duplex complexes; b) homochiral double helix stacks of 1_2Zn^{2+} units and c) crystal packing of double-helix columns: generation a *gearwheels-type* mechanism such that each double helix is in van der Waals contact with four neighbouring ones of the same helical sense.

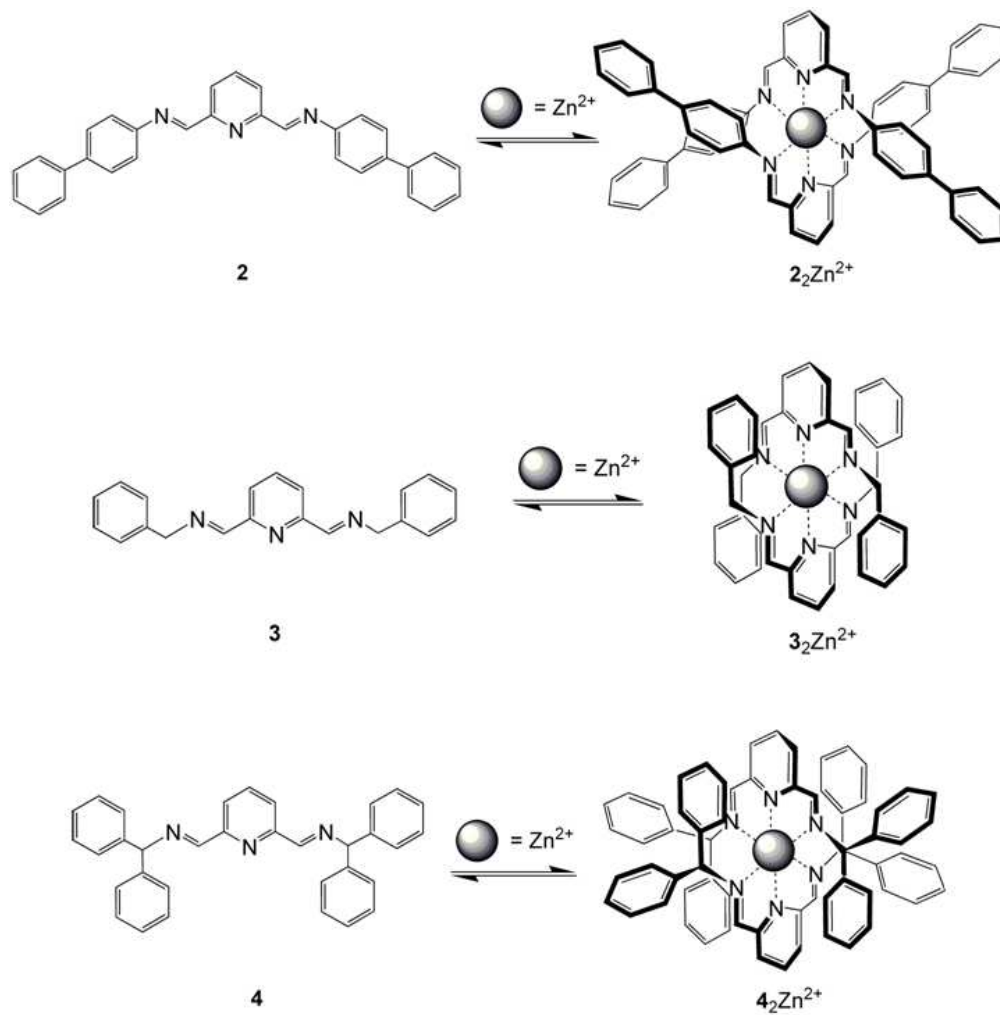
FIGURE 2. Crystal structure in stick representation of the duplex complexes a) 1_2Zn^{2+} , b) 2_2Zn^{2+} , c) 3_2Zn^{2+} and d) 4_2Zn^{2+} ; the Zn^{2+} ions are shown as white spheres.

FIGURE 3 Crystal packing of the duplex complex 2_2Zn^{2+} : a) side view in stick representation and enlarged details of the π - π stacking interactions; b) The square packing arrangement of duplex subunits with the triflate anions in CPK representation filling the central cavity of the resulted tubular channels. The Zn^{2+} ions are shown as gray spheres.

FIGURE 4. Crystal packing in stick representation of the duplex complex 3_2Zn^{2+} .

FIGURE 5 Crystal packing of the duplex complex 4_2Zn^{2+} : a) side view in CPK representation of triangle like trimers and enlarged details of the “diphenylmethane embrace motif”; b) The packing arrangement of homochiral triangle enantiomers: top view of tetrahedral nodes and side view in CPK representation of face-to-face triangle self-assembly.

SCHEME 1. Synthesis of 2_2Zn^{2+} , 3_2Zn^{2+} and 4_2Zn^{2+} duplex complexes



SCHEME 1 Synthesis of 2_2Zn^{2+} , 3_2Zn^{2+} and 4_2Zn^{2+} duplex complexes
190x194mm (96 x 96 DPI)

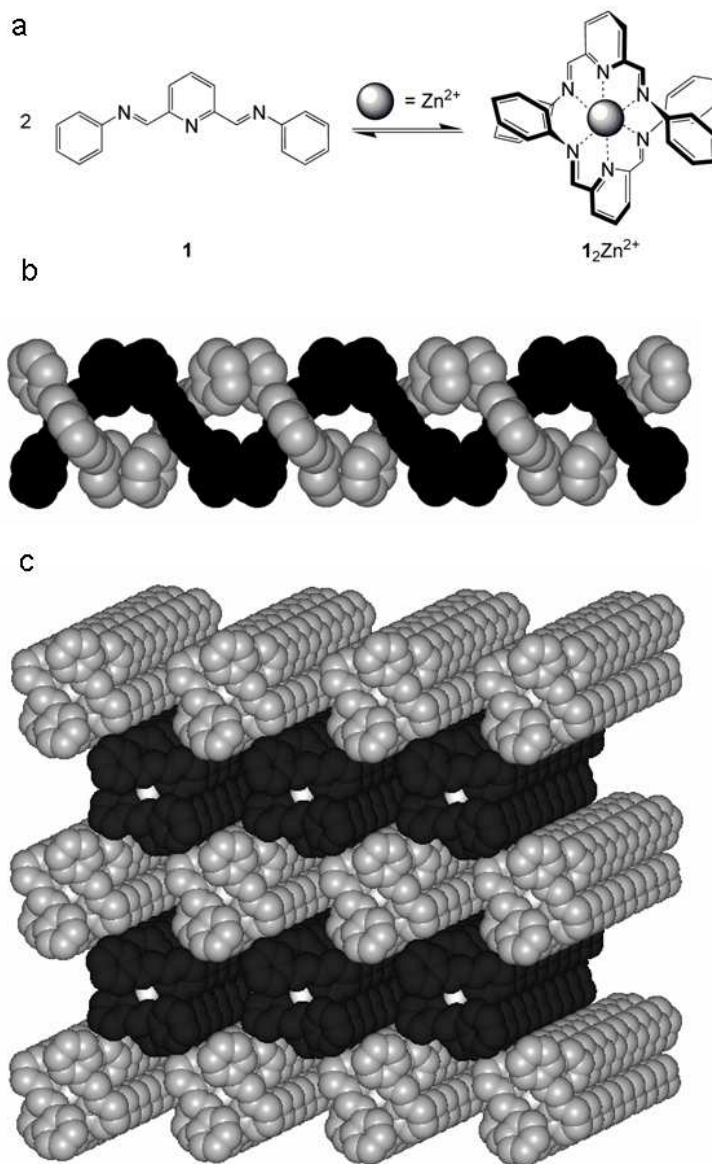


FIGURE 1. From achiral ligands to metallocupramolecular homochiral double helical strands. a) Synthesis of 1_2Zn^{2+} duplex complexes; b) homochiral double helix stacks of 1_2Zn^{2+} units and c) crystal packing of double-helix columns: generation a gearwheels-type mechanism such that each double helix is in van der Waals contact with four neighbouring ones of the same helical sense. 151x245mm (96 x 96 DPI)

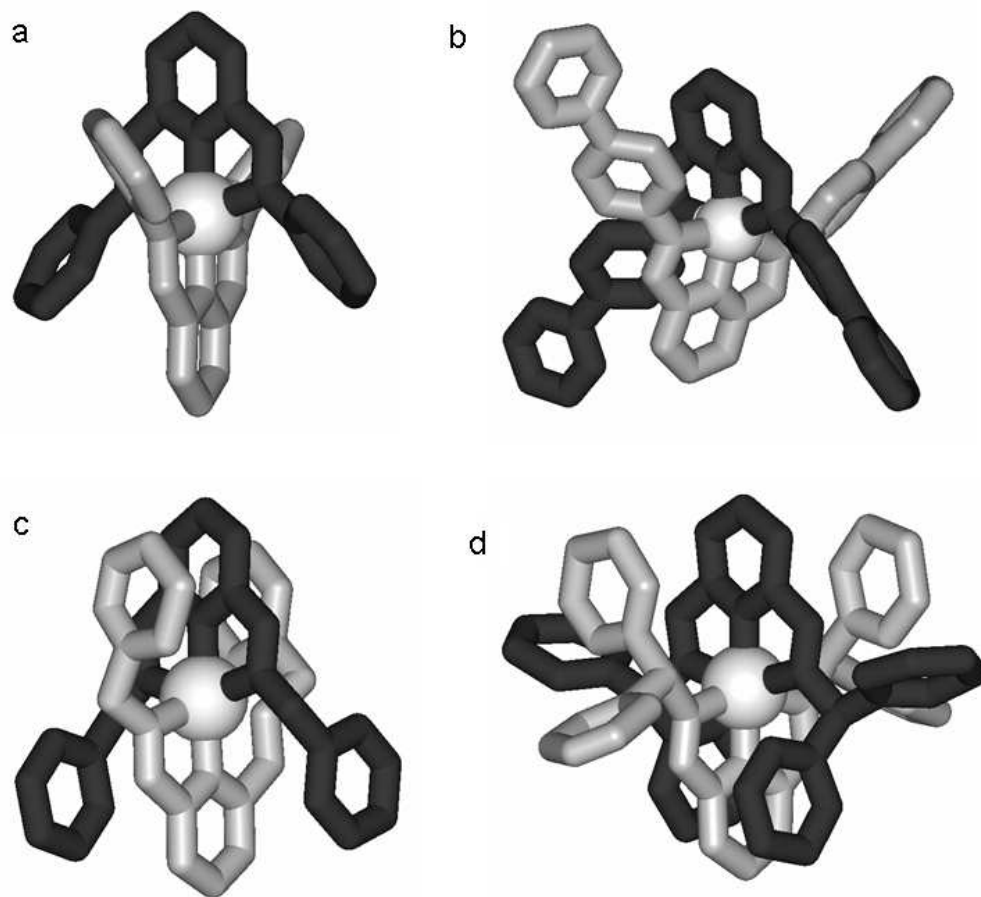


FIGURE 2. Crystal structure in stick representation of the duplex complexes a) 12Zn²⁺, b) 22Zn²⁺, c) 32Zn²⁺ and d) 42Zn²⁺; the Zn²⁺ ions are shown as white spheres.
190x182mm (96 x 96 DPI)

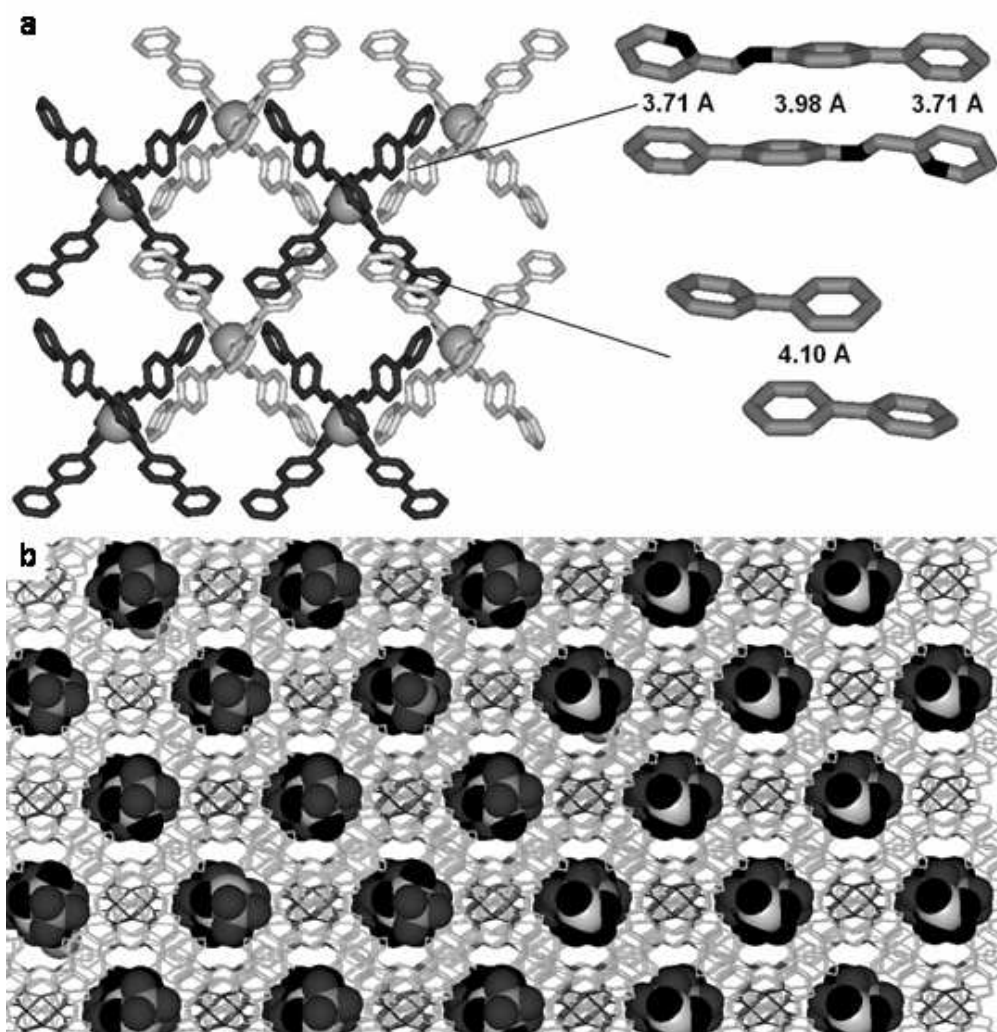


FIGURE 3 Crystal packing of the duplex complex 22Zn²⁺: a) side view in stick representation and enlarged details of the π - π stacking interactions; b) The square packing arrangement of duplex subunits with the triflate anions in CPK representation filling the central cavity of the resulted tubular channels. The Zn²⁺ ions are shown as gray spheres.
142x149mm (96 x 96 DPI)

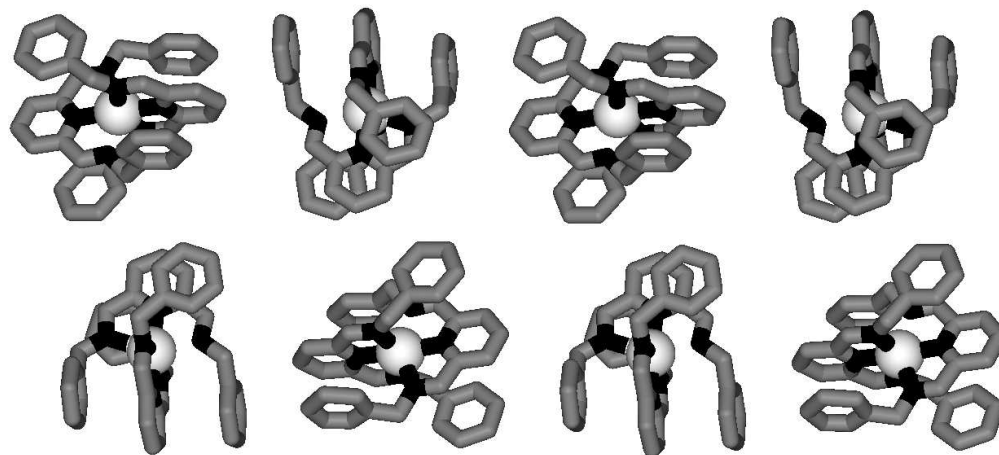


FIGURE 4 Crystal packing in stick representation of the duplex complex 32Zn^{2+} .
325x160mm (96 x 96 DPI)

Review Only

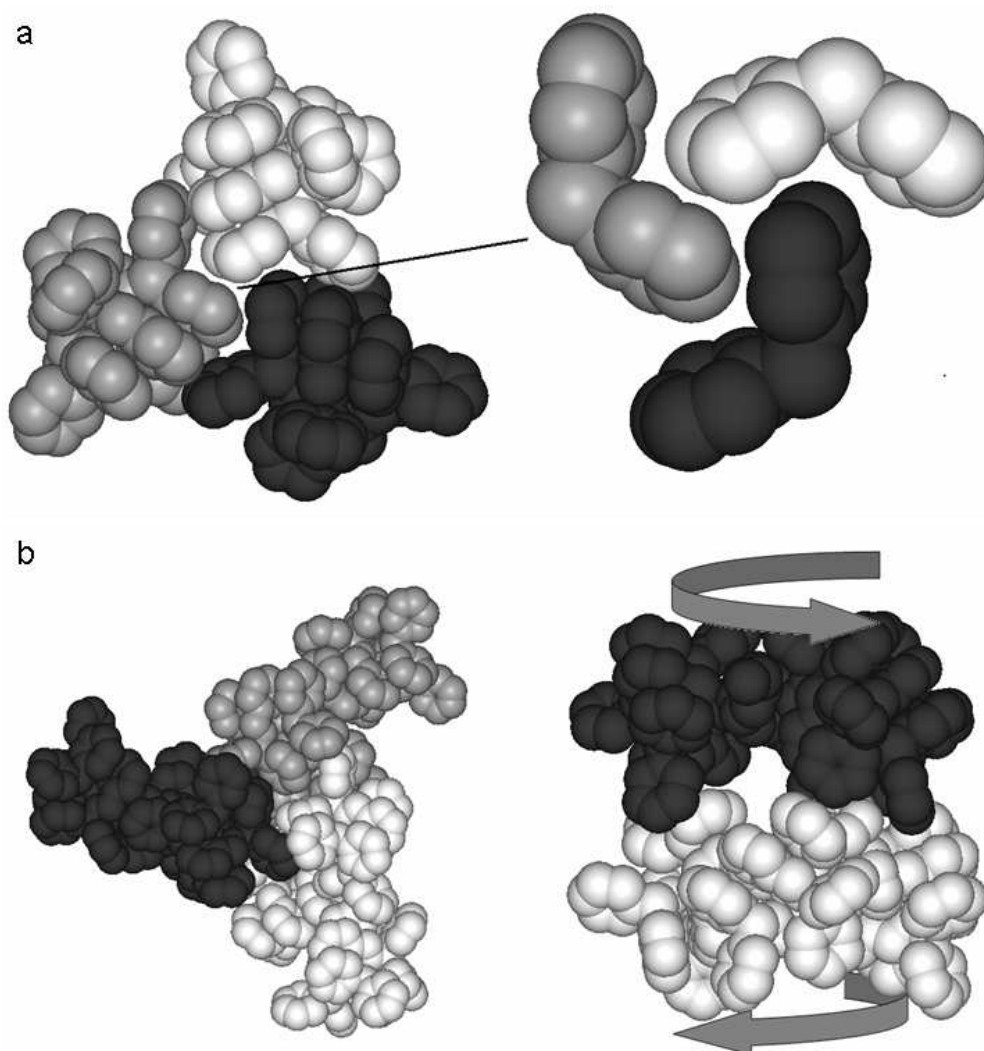


FIGURE 5 Crystal packing of the duplex complex $42Zn^{2+}$: a) side view in CPK representation of triangle like trimers and enlarged details of the Å diphenylmethane embrace motif; b) The packing arrangement of homochiral triangle enantiomers: top view of tetrahedral nodes and side view in CPK representation of face-to-face triangle self-assembly.
190x205mm (96 x 96 DPI)

1
2
3
4
5
6
7

Interpenetrated Constitutional Networks of Aromatic Metallosupramolecular Duplexes

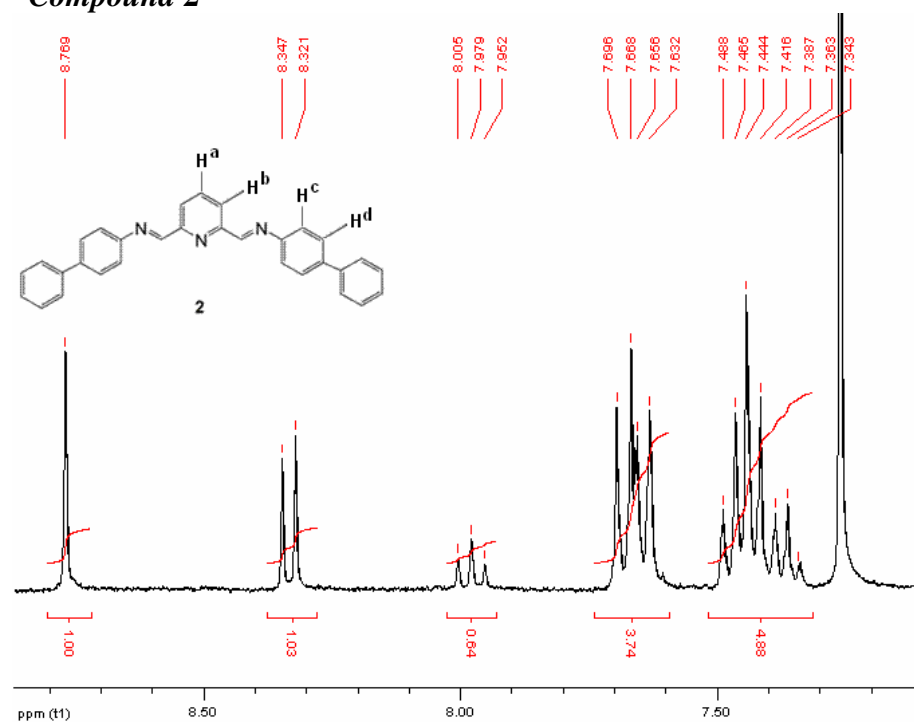
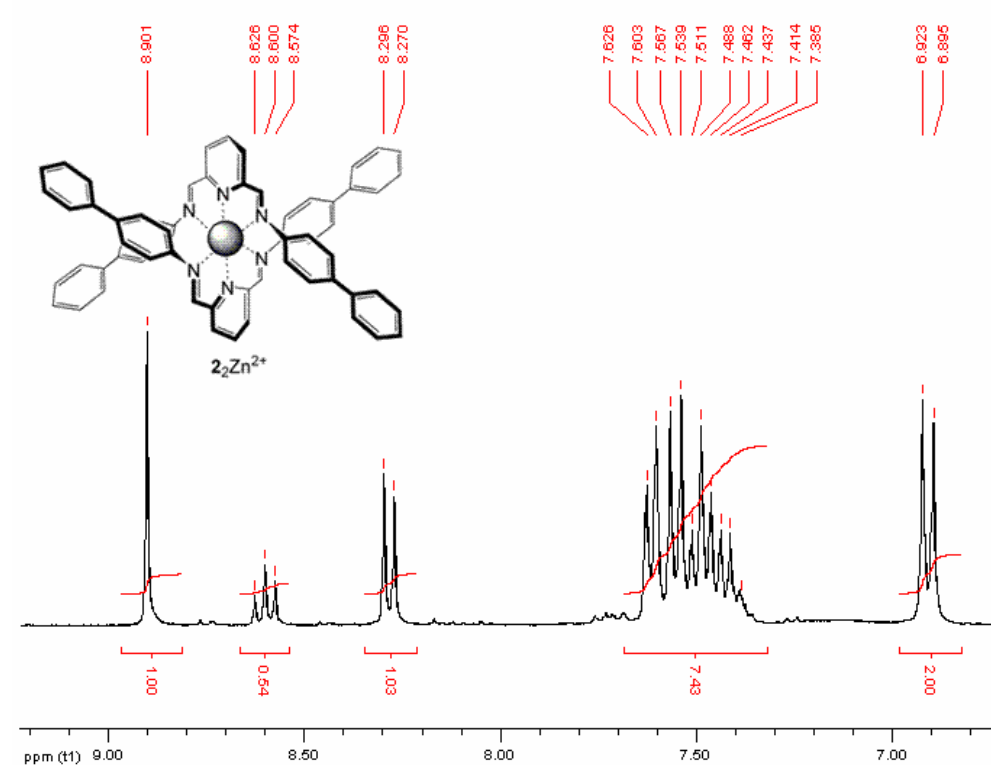
8 Y.-M. LEGRAND^a, F. DUMITRU^{a, b}, A. V. D. LEE^a & M. BARBOIU^{a,*}
9

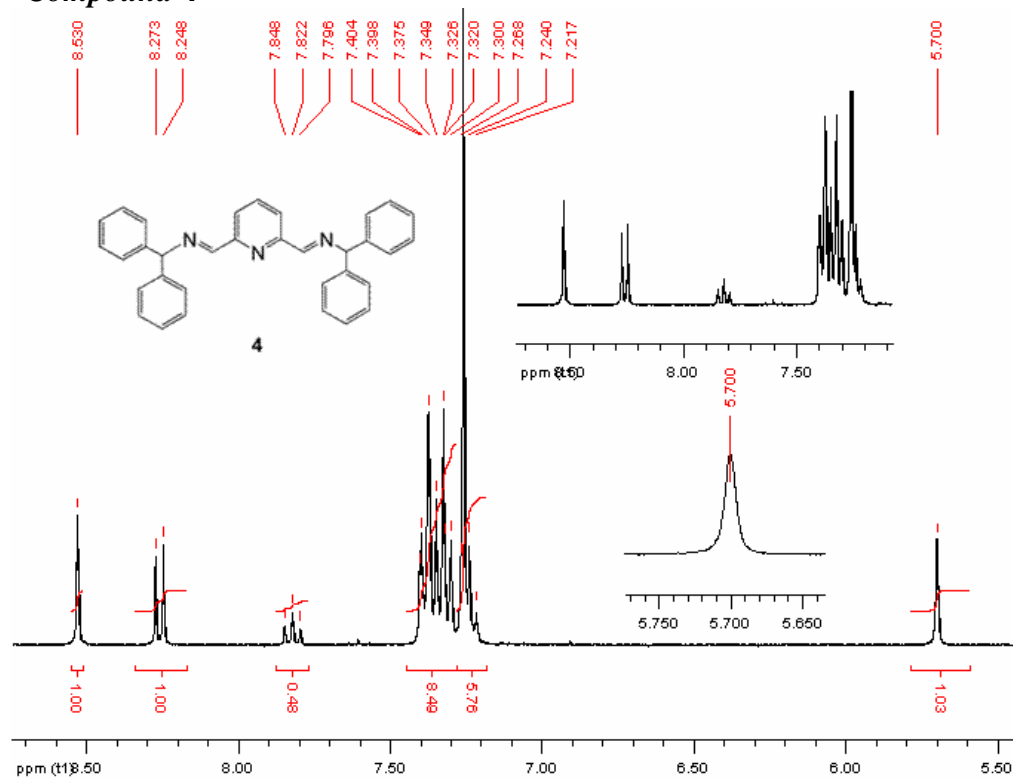
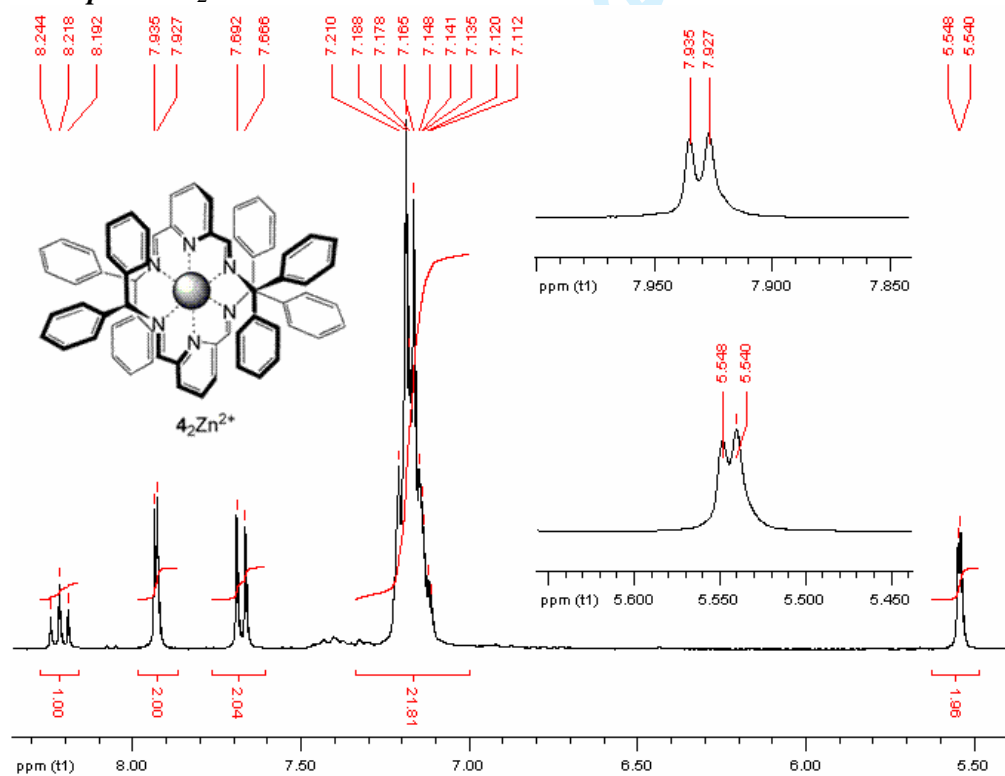
10 ^a*Institut Européen des Membranes, Adaptive Supramolecular Nanosystems Group - ENSCM-*
11 *UMII-CNRS UMR- 5635, Place Eugène Bataillon, CC 047, F-34095 Montpellier, Cedex 5,*
12 *France, ^bUniversity “Politehnica” of Bucharest, Department of Inorganic Chemistry, 1,*
13 *Polizu st., RO-011061 Bucharest, Romania¹*
14
15

16
17
18 E-mail: mihai.barboiu@iemm.univ-montp2.fr
19
20
21
22
23
24

Supplementary Material

25
26
27
28
29
30
31
32
33
34
35
36
37
38
39
40
41
42
43
44
45
46
47
48
49
50
51
52
53
54
55
56
57
58
59
60

$^1\text{H-NMR}$ (ppm) Spectra:***Compound 2**Figure 1S. $^1\text{H-NMR}$ spectrum of **2** in CDCl_3 at RT.***Compound 2_2Zn^{2+}** Figure 2S. $^1\text{H-NMR}$ spectrum of 2_2Zn^{2+} in CD_3CN at RT.

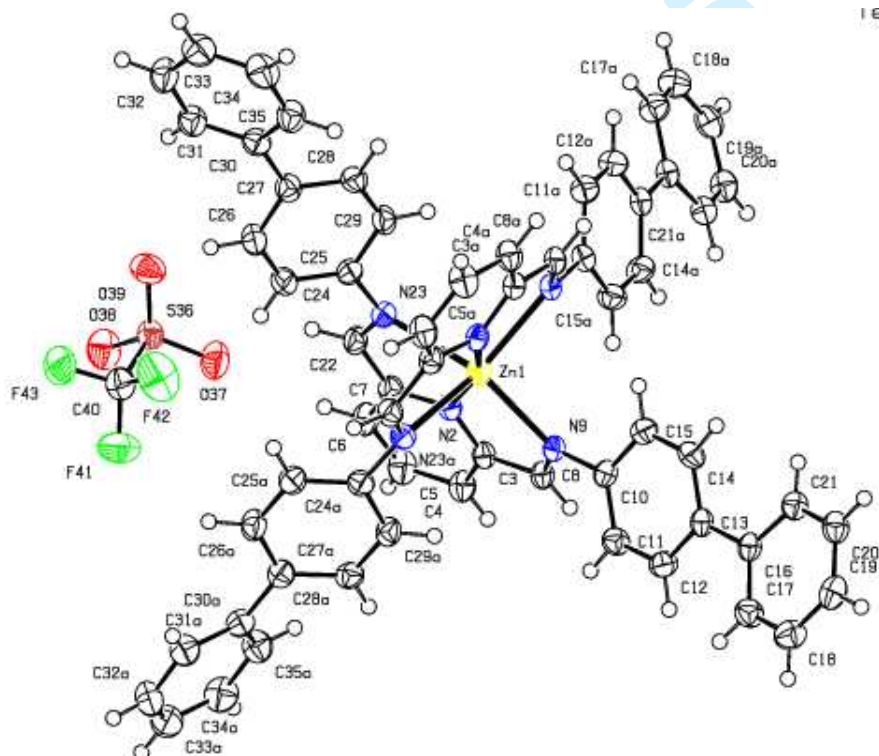
Compound 4**Figure 3S. ¹H NMR spectrum of **4** in CDCl₃ at RT.Compound 4₂Zn²⁺**Figure 4S. ¹H NMR spectrum of **4₂Zn²⁺** in CD₃CN at RT.

Crystallographic Data 2_2Zn^{2+} in C2/c

Formula	C ₆₄ H ₂₆ F ₆ N ₆ O ₆ S ₂ Zn ₁		
Crystal Class	Monoclinic	Space Group	C 1 2/c 1
a	23.6043(4)	alpha	90
b	15.1311(3)	beta	90.8703(16)
c	15.5706(3)	gamma	90
Volume	5560.54(18)	Z	8
Radiation type	Cu K α	Wavelength	1.541800
Dx	1.48	Mr	619.30
Mu	2.004	Temp (K)	175
Size	0.05x 0.11x 0.11		
Colour	yellow	Shape	prismatic
Diffractometer type	XCALIBUR	Scan type	OMEGA
Absorption type	multi-scan	Transmission range	0.80 0.90
Reflections meas.	19534	Independent reflect.	4033
Rint	0.0004	Theta max	61.13
Hmin, Hmax	-26 25		
Kmin, Kmax	-13 16		
Lmin, Lmax	-17 16		

Refinement on F²

R-factor	0.038	Weighted R-factor	0.074
Max shift/su	0.0002		
Delta Rho min	-0.37	Delta Rho max	0.43
Reflections used	3010	sigma(I) limit	2.00
Number of par	384	Goodness of fit	1.036



3₂Zn²⁺ in P 21/c

Formula	C44 H38 F6 N6 O6 S2 Zn1		
Crystal Class	Monoclinic	Space Group	P 1 21/c 1
a	17.854	alpha	90
b	14.078	beta	111.72
c	18.612	gamma	90
Volume	4345.9712(3)	Z	4
Radiation type	Mo K α	Wavelength	0.710730
Dx	1.51	Mr	990.32
Mu	0.743	Temp (K)	175
Size	0.09x 0.11x 0.17		
Colour	yellow	Shape	prismatic
Diffractometer type	XCALIBUR	Scan type	OMEGA
Absorption type	multi-scan	Transmission range	0.92 0.94
Reflections meas.	85283	Independent reflect.	14420
Rint	0.0012	Theta max	32.57
Hmin, Hmax	-26 26		
Kmin, Kmax	-20 20		
Lmin, Lmax	-27 27		

Refinement on F

R-factor	0.049	Weighted R-factor	0.044
Max shift/su	0.0384		
Delta Rho min	-0.46	Delta Rho max	0.81
Reflections used	4862	sigma(I) limit	2.00
Nb of parameters	586	Goodness of fit	1.137

